

THE HADRONIC PICTURE OF THE RADIOGALAXY M87

A. MARINELLI^{†1}, N. FRAIJA^{††2} AND B. PATRICELLI²

Draft version November 3, 2014

ABSTRACT

Very high energy gamma-ray emission of Fanaroff-Riley I objects is not univocally explained by a single emission model. Leptonic models with one and multi-zone emission regions, occurring in the jet of these objects, are usually used to describe the broadband spectral energy distribution. A correlation between the X-ray and TeV emission is naturally expected within leptonic models whereas a lack of correlation between these two observables represents a challenge and favors the hadronic scenarios. This is the case of M87 as we show here by analyzing its TeV and X-ray emission recorded in the last decade. Furthermore, we point out that the spectra obtained by MAGIC, H.E.S.S. and VERITAS telescopes cannot be described with the same leptonic model introduced by the Fermi-LAT collaboration. We introduce hadronic scenarios to explain the TeV gamma-ray fluxes of this radiogalaxy as products of Fermi-accelerated protons interacting with seed photons in the jet or thermal particles in the giant lobes. By fitting this part of spectral energy distribution as pion decay products, we obtain the expected neutrino counterpart and the luminosity of accelerating protons in the jet and/or lobes. With the expected neutrino fluxes we investigate, through Monte Carlo simulations, the possibility to see the signal from M87 with a Km³ neutrino telescope, and compare the results with what has been seen by IceCube experiment up to now. Finally we constrain the features of giant lobes through the observations performed at ultra high energies by TA experiment.

Subject headings: Key words: general – acceleration of particles galaxies: active – galaxies: individual (M87) – radiation mechanisms: non-thermal

1. INTRODUCTION

The nearby radio galaxy M87 is located in the Virgo galaxy cluster at a distance of ~ 16 Mpc ($z=0.0043$) and hosts a central black hole of $(3.2 \pm 0.9) \times 10^9$ solar masses (Mei et al. 2007). M87, being one of the nearest radiogalaxies, is among the best-studied of its class. It has been detected at energy ranges from radio to very high energy (VHE) gamma-rays (Abramowski et al. 2012). The radio emission of M87 comes from the inner lobes, the intermediate ridges and the outer diffuse “halo”, respectively at distances of ~ 2.5 kpc (30”), ~ 15 kpc (3”) and ~ 40 kpc (8”) from the nucleus (Young et al. 2002). The gamma-ray emission of M87 has been detected by Large Area Telescope (LAT) at MeV- GeV energy ranges (Abdo 2009). The entire spectral energy distribution (SED), including the radio, the X-ray (Sparks et al. 1996; Tan et al. 2008), the Chandra and VLBA measurements (Biretta et al. 1991; Despringre et al. 1996) and the LAT gamma-ray data (Abdo 2009), is well fitted with a single-zone Self Synchrotron Compton (SSC) emission model as showed by the Fermi-LAT collaboration (Abdo 2009). In this work we extend the analysis of the SED up to higher energies considering also the data collected by H.E.S.S., MAGIC and VERITAS (Abramowski et al. 2012; Acciari 2010; Aharonian 2006) between 2004 and 2010. The TeV gamma-ray data obtained from these Imaging Atmospheric Cherenkov Telescopes (IACTs) data cannot be explained by the same SSC scenario so that additional mechanisms should be considered to explain the whole spectrum (for example hadronic processes; (Fraija et al. 2012a) or multi-zone SSC). Here we investigate two different hadronic scenarios to describe the TeV gamma-ray data: the interaction of accelerated protons in the jet of M87 with the MeV SSC photons and the interaction of boosted protons in the giant lobes (Fraija 2014a) with the thermal protons target. The individual SEDs obtained with H.E.S.S., MAGIC and VERITAS campaigns have been well fitted considering the proton-proton (pp) and the proton-gamma ($p\gamma$) scenarios with different sets of spectral parameters. We also compared simultaneous activities in gamma-rays (with the above mentioned data) and in X-rays, with data from RXTE-ASM (Swank 2006) on different time scales. The emission in these two energy bands resulted not significantly correlated providing further hints of hadronic origin of the TeV gamma-rays observed. Given these results, we consider the possibility of having a neutrino counterpart emitted by M87 and we obtain the expected neutrino spectra from the best fit gamma-ray spectra of the three different data samples. We introduce the obtained neutrino spectra in a Monte Carlo simulation of a hypothetical Km³ neutrino telescope in the north hemisphere and we get the signal to noise ratio for one year of data-taking. Since the observation of M87 with a neutrino telescope cannot be considered preferential from one of the two hemispheres, it has been possible to compare this result with what has been observed up to now by the IceCube experiment. Finally, within the presented hadronic scenario we investigate the possibility for protons to be accelerated up to Ultra High Energies (UHEs) and put limits on the density of M87 giant lobes considering different sizes. For this calculation, we use the accelerated proton spectra obtained through the spectral fit of TeV gamma-ray (within the pp interaction scenario). Then, we constrained the properties of the lobes taking into account the UHE proton flux observed by Telescope Array (TA) experiment (Abu-Zayyad & et al. 2012) in 5 years of data-taking.

antonio.marinelli@fisica.unam.mx, nifraija@astro.unam.mx and bpatricelli@astro.unam.mx

¹ Instituto de Física, Universidad Nacional Autónoma de México, Circuito Exterior, C.U., A. Postal 70-264, 04510 México D.F., México.

² Instituto de Astronomía, Universidad Nacional Autónoma de México, Circuito Exterior, C.U., A. Postal 70-264, 04510 México D.F., México.

[†] Actually at I.N.F.N. and Physics Institute of Pisa University, Edificio C - Polo Fibonacci Largo B. Pontecorvo, 3 - 56127 Pisa, Italy.

^{††} Luc Binette-Fundación UNAM Fellow.

2. HADRONIC INTERACTIONS

Radiogalaxies have been proposed as powerful accelerators of charged particles through the Fermi acceleration mechanism (Rieger et al. 2007). The Fermi-accelerated protons can be described by a simple power law

$$\frac{dN_p}{dE_p} = A_p E_p^{-\alpha}, \quad (1)$$

where α is the power index and A_p is the proportionality constant. For this work, we consider that these protons are cooled down by $p\gamma$ and pp interactions occurring in the jet and giant lobes, respectively. Both interactions produce VHE gamma-rays and neutrinos as explained in the following subsections. We hereafter use primes (unprimes) to define the quantities in a comoving (observer) frame, $c=\hbar=1$ in natural units and redshift $z \simeq 0$.

2.1. $p\gamma$ interaction

Charged (π^+) and neutral (π^0) pions are obtained from $p\gamma$ interaction through the following channels

$$p\gamma \longrightarrow \Delta^+ \longrightarrow \begin{cases} p\pi^0 & \text{fraction } 2/3, \\ n\pi^+ & \text{fraction } 1/3, \end{cases} \quad (2)$$

and neutral pions decay into photons, $\pi^0 \rightarrow \gamma\gamma$, carrying 20% ($\xi_{\pi^0} = 0.2$) of the proton's energy E_p . As has been pointed out by Waxman and Bahcall (Waxman & Bahcall 1997), the photo-pion spectrum is obtained from the efficiency of this process

$$f_{\pi^0, p\gamma} \simeq \frac{t'_{dyn}}{t'_{\pi^0}} = \frac{r_d}{2\delta_D \gamma_p^2} \int d\epsilon \sigma_\pi(\epsilon) \xi_{\pi^0} \epsilon \int dx x^{-2} \frac{dn_\gamma}{d\epsilon_\gamma}(\epsilon_\gamma = x), \quad (3)$$

where t'_{dyn} and t'_{π^0} are the dynamical and the pion cooling times, γ_p is the proton Lorentz factor, $r_d = \delta_D dt$ is the comoving dissipation radius as function of Doppler factor (δ_D) and observational time (t^{obs}), $dn_\gamma/d\epsilon_\gamma$ is the spectrum of target photons, $\sigma_\pi(\epsilon_\gamma) = \sigma_{peak} \approx 9 \times 10^{-28} \text{ cm}^2$ is the cross section of pion production. Solving the integrals we obtain

$$f_{\pi^0, p\gamma} \simeq \frac{L_\gamma \sigma_{peak} \Delta\epsilon_{peak} \xi_{\pi^0}}{8\pi \delta_D^2 r_d \epsilon_{\gamma, b} \epsilon_{peak}} \begin{cases} \left(\frac{\epsilon_{\pi^0, \gamma, c}}{\epsilon_0}\right)^{-1} \left(\frac{\epsilon_{\pi^0, \gamma}}{\epsilon_0}\right) & \epsilon_{\pi^0, \gamma} < \epsilon_{\pi^0, \gamma, c} \\ 1 & \epsilon_{\pi^0, \gamma, c} < \epsilon_{\pi^0, \gamma}, \end{cases} \quad (4)$$

where $\Delta\epsilon_{peak}=0.2 \text{ GeV}$, $\epsilon_{peak} \simeq 0.3 \text{ GeV}$, L_γ is the luminosity and $\epsilon_{\gamma, b}$ is the break energy of the seed photon field (Fraija 2014b). By considering the simple power law for a proton distribution (eq. 1) and the conservation of the photo pion flux for this process, $f_{\pi^0, p\gamma} E_p (dN/dE)_p dE_p = \epsilon_{\pi^0, \gamma} (dN/d\epsilon)_{\pi^0, \gamma} d\epsilon_{\pi^0, \gamma}$, the photo-pion spectrum is given by

$$\left(\epsilon^2 \frac{dN}{d\epsilon}\right)_{\pi^0, \gamma} = A_{p\gamma, \gamma} \begin{cases} \left(\frac{\epsilon_{\pi^0, \gamma, c}}{\epsilon_0}\right)^{-1} \left(\frac{\epsilon_{\pi^0, \gamma}}{\epsilon_0}\right)^{-\alpha+3} & \epsilon_{\pi^0, \gamma} < \epsilon_{\pi^0, \gamma, c} \\ \left(\frac{\epsilon_{\pi^0, \gamma}}{\epsilon_0}\right)^{-\alpha+2} & \epsilon_{\pi^0, \gamma, c} < \epsilon_{\pi^0, \gamma}, \end{cases} \quad (5)$$

with the normalization energy ϵ_0 , proportionality constant of $p\gamma$ interaction given by

$$A_{p\gamma, \gamma} = \frac{L_\gamma \epsilon_0^2 \sigma_{peak} \Delta\epsilon_{peak} \left(\frac{2}{\xi_{\pi^0}}\right)^{1-\alpha}}{4\pi \delta_D^2 r_d \epsilon_{\gamma, b} \epsilon_{peak}} A_p, \quad (6)$$

and the break photon-pion energy given by

$$\epsilon_{\pi^0, \gamma, c} \simeq 31.87 \text{ GeV } \delta_D^2 \left(\frac{\epsilon_{\gamma, b}}{\text{MeV}}\right)^{-1}. \quad (7)$$

The eq. 5 describes the contribution of photo-pion emission to the SED.

2.2. pp interaction

π^+ and π^0 are also obtained from the pp interaction by means of channel (Becker 2008; Atoyan & Dermer 2003; Dermer & Menon 2009; Aharonian 2002)

$$p + p \longrightarrow \pi^+ + \pi^- + \pi^0 + X. \quad (8)$$

Once again neutral pions decay in two gammas, $\pi^0 \rightarrow \gamma\gamma$, carrying 33% ($\xi_{\pi^0}=0.33$) of the proton energy E_p . Assuming that accelerated protons interact in the lobe region, spatially constrained by R and thermal particle density n_p , we describe the efficiency of the process through

$$f_{\pi^0, pp} \approx R n_p k_{pp} \sigma_{pp}, \quad (9)$$

where $\sigma_{pp} \simeq 30(0.95 + 0.06 \ln(E/\text{GeV}))$ mb is the nuclear interaction cross section and $k_{pp} = 1/2$ is the inelasticity coefficient. Taking into account the proton distribution (eq. 1) and the conservation of the photo pion flux (Atoyan & Dermer 2003; Fraija et al. 2012b; Aharonian 2002; Hardcastle et al. 2009)

$$f_{\pi^0, pp}(E_p) E_p \left(\frac{dN_p}{dE_p} \right)^{obs} dE_p = \epsilon_{\gamma, \pi^0} \left(\frac{dN_\gamma}{d\epsilon_\gamma} \right)^{obs}_{\pi^0} d\epsilon_{\gamma, \pi^0}, \quad (10)$$

then the observed gamma-ray spectrum can be written as

$$\left(\epsilon_\gamma^2 \frac{dN_\gamma}{d\epsilon_\gamma} \right)^{obs}_{\pi^0} = A_{pp, \gamma} \left(\frac{\epsilon_{\gamma, \pi^0}}{\epsilon_0} \right)^{2-\alpha}, \quad (11)$$

where the proportionality constant of pp interaction is

$$A_{pp, \gamma} = R n_p k_{pp} \sigma_{pp} (2/\xi_{\pi^0})^{2-\alpha} \epsilon_0^2 A_p. \quad (12)$$

The eq. 11 shows the contribution of pp interactions to the spectrum of gamma rays produced in the lobes.

3. THE VHE NEUTRINO EXPECTATION

The hadronic interactions described above produce also a neutrino counterpart in the jet (through $p\gamma$) and in the lobes (through pp) of the AGN. In these processes the neutral pion produced decays into two gammas, $\pi_0 \rightarrow \gamma\gamma$, and the charged pion into leptons and neutrinos, $\pi^\pm \rightarrow e^\pm + \nu_\mu/\bar{\nu}_\mu + \bar{\nu}_\mu/\nu_\mu + \nu_e/\bar{\nu}_e$. The effect of neutrino oscillations on the expected flux balances the number of neutrinos per flavor (Becker 2008) arriving to Earth. Assuming the described interactions, we expect that the VHE gamma rays and the respective neutrino counterpart have a SED strictly linked to the SED of accelerated primary protons. The spectrum of neutrino produced by the hadronic interactions can be written as:

$$\frac{dN_\nu}{dE_\nu} = A_\nu \left(\frac{E_\nu}{\text{TeV}} \right)^{-\alpha_\nu}, \quad (13)$$

where the normalization factor, A_ν , is calculated by correlating the neutrino flux luminosity with the TeV photon flux (Becker 2008). This correlation is given by:

$$\int \frac{dN_\nu}{dE_\nu} E_\nu dE_\nu = K \int \frac{dN_\gamma}{dE_\gamma} E_\gamma dE_\gamma. \quad (14)$$

Where for pp interaction should be used $K = 1$ and for $p\gamma$ interaction $K = 1/4$ (see, Julia Becker Halzen 2007, and reference therein). The spectral indices for neutrino and gamma-ray spectrum are considered similar $\alpha \simeq \alpha_\nu$ (Becker 2008) while the carried energy is slightly different: each neutrino brings 5% of the initial proton energy ($E_\nu = 1/20 E_p$) while each photon brings around 16.7%. With these considerations the normalization factors are related by

$$A_{(pp, \nu/p\gamma, \nu)} = K \cdot A_{(pp, \gamma/p\gamma, \gamma)} \epsilon_0^{-2} (2)^{-\alpha+2}, \quad (15)$$

where $A_{pp, \gamma}$ and $A_{p\gamma, \gamma}$ are given by the Eq. (12) and the Eq. (6) and the factor $2^{-\alpha+2}$ is introduced because the neutrino carries 1/2 of γ energy. Therefore extending the spectrum of expected neutrino to maximum energies detectable by a Km^3 Cherenkov detector array, we can obtain the number expected neutrino events detected as:

$$N_{ev} \approx T \rho_{water/ice} N_A V_{eff} \int_{E_{min}}^{E_{max}} \sigma_\nu A_{(pp, \nu/p\gamma, \nu)} \left(\frac{E_\nu}{\text{TeV}} \right)^{-\alpha} dE_\nu. \quad (16)$$

Where N_A is the Avogadro number, $\rho_{water/ice}$ is the density of environment for the neutrino telescope, E_{min} and E_{max} are the low and high energy threshold considered, V_{eff} is the $\nu_\mu + \bar{\nu}_\mu$ effective volume, obtained through Monte Carlo simulation, for a hypothetical Km^3 neutrino telescope considering a neutrino source at the declination of M87.

4. UHE COSMIC RAYS PHENOMENOLOGY

As explained before, for this class of AGN two possible acceleration regions have been identified: one close to black-hole (BH) at a sub-parsec distance and the other one in the extended lobes at dozens of kiloparsecs. Relativistic protons could be accelerated up to UHE depending on the properties of the acceleration region: the magnetic field (\mathcal{B}) and the size (\mathcal{R}). Then, the maximum energy obtained from the source is (Hillas 1984)

$$E_{max} = Z e \mathcal{B} \mathcal{R} \Gamma, \quad (17)$$

where the maximum energy reachable is limited in the jet by the emission region ($\mathcal{R} = r_{pc}$) (Abdo 2009), and in the lobes by the magnetic field $\mathcal{B} = B_{\mu G}$ (de Gasperin et al. 2012); with Z we indicate the atomic number.

Taking into account the values of magnetic field and acceleration region in the jet ($B=55$ mG and $r_d=1.4 \times 10^{16}$ cm) (Abdo 2009) and in the lobes ($B=10^{-6}$ Gauss and $R=10$ kpc) (de Gasperin et al. 2012), the maximum energies achievable E_{max} (eq. 17) are 1.05×10^{19} eV and 4.22×10^{20} eV, respectively. From these considerations we can claim that UHECRs can reach energies greater

that 57 EeV only through the lobe regions. On the other hand, UHECRs traveling from source to Earth are randomly deviated by galactic

$$\theta_G \simeq 3.8^\circ \left(\frac{E_{p,th}}{57 \text{ EeV}} \right)^{-1} \int_0^{L_G} \left| \frac{dl}{\text{kpc}} \times \frac{B_G}{4 \mu\text{G}} \right| \quad (18)$$

and extragalactic

$$\theta_{EG} \simeq 4^\circ \left(\frac{E_{p,th}}{57 \text{ EeV}} \right)^{-1} \left(\frac{B_{EG}}{1 \text{ nG}} \right) \left(\frac{L_{EG}}{100 \text{ Mpc}} \right)^{1/2} \left(\frac{l_c}{1 \text{ Mpc}} \right)^{1/2} \quad (19)$$

magnetic fields. Here L_{EG} corresponds to the average path of extragalactic charged particle going through our Galaxy (20 kpc), l_c is the coherence length (Stanev 1997; Moharana & Gupta 2009) and $E_{p,th} = 57 \text{ EeV}$ is the threshold energy of the TA experiment.

4.0.1. Expected Number of UHECRs

TA experiment, located at 1.400 m above sea level in Millard Country, Utah, USA, is built with three fluorescence detector (FD) stations and a scintillator surface detector (SD) array (Abu-Zayyad & et al. 2012). It was designed to observe extensive air showers produced by primary cosmic rays with energies above 1 EeV. This array has an area of $\sim 700 \text{ Km}^2$ and is in data taking since 2008. To estimate the number of UHECRs, we consider the TA exposure for a point source TA exp = $\Xi t_{op} \omega(\delta_s)/\Omega$, with $\Xi \times t_{op} = 5 \text{ yr} \times 7 \times 10^2 \text{ km}^2$. Here t_{op} is the total operational time (from 2008 May 11 and 2013 May 4), $\omega(\delta_s)$ is an exposure correction factor for the declination of Mrk 421 (Sommers 2001) and $\Omega \simeq \pi$ the experiment covered solid angle. The expected number of UHECRs above an energy $E_{p,th}$ yields

$$N_{UHECR} < (\text{TA exp}) \times N_p, \quad (20)$$

where N_p is the UHECR flux arriving to the detector. Taking into account that the proton spectrum is described by eq. (1), then the expected number of UHECRs above a threshold energy $E_{p,th}$ can be written as

$$N_{UHECR} < \frac{\Xi t_{op} \omega(\delta_s)}{\Omega (\alpha - 1)} \text{ GeV} \left(\frac{E_{p,th}}{\text{GeV}} \right)^{-\alpha+1} A_p \quad (21)$$

with α the spectral index and A_p the proportionality constant. These values can be obtained from the signature of hadronic interactions at lower energies.

5. ANALYSIS AND RESULTS

Evidence of hadronic processes occurring in the jet and in lobes of M87 radiogalaxy has been analyzed at the beginning of this work. A first hint of possible hadronic components in the gamma-ray emission of M87 has been obtained with the global spectral analysis of this object. The entire SED of this radiogalaxy was fit by Fermi Collaboration in 2009 with a SSC one-zone model (Abdo 2009). In this work we extend the spectral analysis to the VHE regime with gamma-ray campaigns reported by H.E.S.S. with data collected in 2005-2007 (Beilicke et al. 2008), by VERITAS with data collected in 2008 (Acciari 2010) and by MAGIC with data collected in 2005-2007 (Aleksić & et al. 2012). In particular, we fitted the Fermi-LAT data obtaining the same spectral index reported by the Fermi collaboration and we extended the best fit power law up to the higher energies (see fig. 1). This analysis pointed out the presence of extra components in addition to the single one-zone SSC emission, possibly of hadronic origin. A further evidence of the hadronic origin of these extra components comes from the study of the correlation of these gamma-ray data with the simultaneous X-ray data in the 2-10 keV energy range collected by RXTE/ASM (http://xte.mit.edu/ASM_lc.html). The analysis reported in fig. 2 comprises VERITAS nightly averaged fluxes above 250 GeV, MAGIC fluxes above 100 GeV averaged on different time scales and H.E.S.S. nightly averaged fluxes above 730 GeV. Since for VERITAS data the exact duration of the nightly observation is unknown, we assumed that the gamma-ray fluxes are constant for a whole day and we combined them with RXTE/ASM daily data taken on the same observation days. In the case of MAGIC and H.E.S.S. data, we rebinned the RXTE/ASM daily and dwell⁵ light curves respectively, in order to have X-ray fluxes averaged on the same time intervals as MAGIC and H.E.S.S. Although the data sets can be fitted with a straight line (see fig. 2), all of them are weakly correlated, with low Spearman correlations coefficients (see Table 1). Considering the reported evidences of

γ -experiment	Correlation coefficient	Best fit slope	Reduced χ^2
VERITAS	0.01	$(1.48 \pm 1.58) \times 10^{-12}$	1.81
MAGIC	0.31	$(1.79 \pm 1.23) \times 10^{-12}$	0.47
H.E.S.S.	-0.16	$(-3.52 \pm 2.31) \times 10^{-13}$	0.60

Table 1: Pearson correlation coefficient, slope and reduced χ^2 of the best fitting straight line for the correlations.

hadronic emission components at VHE, we proceeded to describe the gamma-ray spectra of M87 as π^0 decay products occurring in $p\gamma$ and pp interactions. In the $p\gamma$ interaction model, we assumed that these neutral pions are produced in the interaction of Fermi-accelerated protons with the synchrotron self Compton (SSC) photons at $\sim 2 \text{ MeV}$ encountered in the emission region. The gamma-ray spectrum generated by this process (eq. 5) depends on the proton spectrum parameters (through A_p and α), the

⁵ it is referred to a time bin of 90 seconds

comoving dissipation radius r_d , the break energy of target photons $\epsilon_{\gamma,b}$ and the Doppler factor δ_D . We fitted the observed spectra (see fig. 3) with the following function (see also the section 2) where $[A]$ and $[B]$ are the free parameters.

$$\left(\epsilon^2 \frac{dN}{d\epsilon} \right)_{\pi^0, \gamma} = [A] \begin{cases} \left(\frac{\epsilon_{\pi^0, \gamma, c}}{\epsilon_0} \right)^{-1} \left(\frac{\epsilon_{\pi^0, \gamma}}{\epsilon_0} \right)^{-[B]+3} & \epsilon_{\pi^0, \gamma} < \epsilon_{\pi^0, \gamma, c} \\ \left(\frac{\epsilon_{\pi^0, \gamma}}{\epsilon_0} \right)^{-[B]+2} & \epsilon_{\pi^0, \gamma, c} < \epsilon_{\pi^0, \gamma}, \end{cases} \quad (22)$$

	Parameter	Symbol	H.E.S.S.	MAGIC	VERITAS
Proportionality constant (10^{-13} TeV/cm ² /s)	[A]	$A_{p\gamma, \gamma}$	13.3 ± 0.096	3.38 ± 0.431	5.39 ± 0.94
Power index	[B]	α	2.28 ± 0.052	2.97 ± 0.121	2.70 ± 0.23
Chi-square/d.o.f		$\chi^2/\text{d.o.f}$	14.62/7	12.59/4	4.794/4

Table 2: the best fit of the set of $p\gamma$ interaction obtained after fitting the VHE spectrum.

In the pp interaction model, we have considered accelerated protons described by the simple power law (eq. 1) which could be accelerated in the lobes and furthermore interact with thermal particles present there. The spectrum generated by this process (eq. 23) depends on the proton spectrum parameters (through A_p and α), the proton luminosity (through A_p), number density of thermal particles and size of the lobes. We fitted the observed spectra (see fig. 3) with the following function (see also the section 2) with the free parameters $[A]$ and $[B]$.

$$\left(\epsilon_\gamma^2 \frac{dN_\gamma}{d\epsilon_\gamma} \right)_{\pi^0}^{obs} = [A] \left(\frac{\epsilon_{\gamma, \pi^0}}{\text{GeV}} \right)^{2-[B]}, \quad (23)$$

	Parameter	Symbol	H.E.S.S.	MAGIC	VERITAS
Proportionality constant (10^{-13} TeV/cm ² /s)	[A]	$A_{pp, \gamma}$	12.0 ± 0.08	4.00 ± 0.43	5.11 ± 0.89
Power index	[B]	α	2.22 ± 0.05	2.33 ± 0.12	2.48 ± 0.20
Chi-square/d.o.f.		$\chi^2/\text{d.o.f.}$	13.93/7	7.28/4	3.60/4

Table 3: the best fit of the set of pp interaction obtained after fitting the VHE spectrum.

The parameters obtained with the explained fits (Tables 2 and 3) were used in this work to obtain the expected neutrino spectral parameters ($A_{(pp, \nu/p\gamma, \nu)}$, α). Being M87 a close source, no extragalactic background light (EBL) absorption models (Rae & Mazin 2008) were considered relating $A_{(pp, \gamma/p\gamma, \gamma)}$ to $A_{(pp, \nu/p\gamma, \nu)}$. Convoluting the obtained parameters with the effective volume (V_{eff}) of a hypothetical Km³ neutrino telescope located in the northern hemisphere it was possible to obtain the expected neutrino events. M87 position was considered in the Monte Carlo simulation as a neutrino emitters with no cut-off for the neutrino spectra in the sensible energy range (10 GeV-10 PeV). For the simulated neutrino telescope we calculated also the atmospheric and cosmic neutrinos expected from the portion of the sky inside a cone centered in M87 and having an open angle of 1°. The cosmic diffuse neutrinos signal has been discussed by Waxman and Bahcall (Bahcall & Waxman 2001; Waxman 1998) and the upper limit for this flux is $E_\nu^2 d\Phi/dE_\nu < 2 \times 10^{-8} \text{ GeV cm}^{-2} \text{ s}^{-1} \text{ sr}^{-1}$ (Waxman & Bahcall 1999). The atmospheric neutrino flux is well described by the Bartol model (Barr et al. 2004, 2006) for the range of energy considered in this analysis. The atmospheric muon “background” was precluded from this analysis due to earth filtration and to the softer spectrum with respect to the neutrino signal and “backgrounds” considered. The signal to noise ratio was obtained taking into account one year of observations for the considered neutrino telescope. No visible excess of M87 neutrino signal was encountered (see fig.4) for the two hadronic models (pp and $p\gamma$) applied to the considered spectra (see fig.3). Only neutrino flux obtained with the hadronic fit (pp) of H.E.S.S. data has the possibility to be detected in several years of observation with a global neutrino network⁶ (GNN). This future scenario will be possible considering the declination of M87 and the favorable cross correlation between IceCube and a future northern Km³ neutrino telescope. Linking the fit obtained for VHE gamma-ray with the accelerating proton spectra we finally estimate the UHECRs luminosity of M87. In accordance with the proposed model, we took into account a proton flux constrained by the pp interactions occurring in the lobes of M87 and set upper limits on the number of UHECRs in agreement with the 5 years of observations performed by TA experiment. Taking into account the uncertainties on UHECRs arrival direction explained in section 4 and the numerical approach (Ryu et al. 2010) available for extragalactic sources, we considered two contour regions of 5° and 10° around the only UHECR possibly related to M87 position (as shown in fig. 6). With the assumption of less than one event detected in 5 years and the obtained opacity on UHE proton flux produced by pp interaction we calculated the lower limits of thermal proton density for different sizes of the M87, as shown in fig. 5. From this figure one can see that for the lobe size $1 \text{ kpc} < R < 100 \text{ kpc}$ the expected thermal proton density lies in the range $10^{-8} \text{ cm}^{-3} < n_p < 10^{-3} \text{ cm}^{-3}$.

6. CONCLUSIONS

The radiogalaxy M87 was observed in the last decade at VHEs by several IACTs. The nature of the emission in this energy range is still under debate. In this work we extended previous analysis of M87 SED up to VHEs with data collected in the last decade by MAGIC, VERITAS and H.E.S.S. We showed that the SSC one-zone scenario previously published by the Fermi collaboration cannot be used to describe the VHE part of the SED within the same leptonic model, therefore opening the possibility for extra hadronic components. Further evidences for a non-leptonic origin of the selected gamma-ray data come from the correlation of gamma-ray fluxes with simultaneous X-ray data collected by RXTE/ASM. The samples considered in these

⁶ Global network of neutrino telescopes (IceCube, KM3NeT, ANTARES and Baikal); a infrastructure of several Km³ and a complete coverage of the sky.

two different energy ranges have been found to be weakly correlated, with very low Spearman correlation coefficients. Given these results we investigated possible hadronic scenarios to explain the VHE emission of M87. We fitted the selected gamma-ray spectra considering proton-photon and proton-proton interactions occurring respectively in the jet and in the lobes of M87. For the first hadronic interaction we considered as target photons those ones at the second SSC peak, while for the second hadronic interaction we considered as a target the thermal protons present in the giant lobes. We verified that the samples of data collected by MAGIC, VERITAS and H.E.S.S. were well fitted by the two hadronic models and we used the best fit parameters to estimate the spectral neutrino counterpart. The found neutrino spectra have been convoluted with the effective volume of a hypothetical northern hemisphere Km^3 neutrino telescope, through Monte Carlo simulations. We obtained the signal to noise ratio for the circular region of one square degree around the position of M87. None of the selected neutrino spectra gave us a considerable neutrino signal excess from M87 respect to the atmospheric and the diffuse extragalactic neutrino event rates. These results have been found in accordance with what has been observed in four years of IceCube data-taking. However, the neutrino spectrum obtained from the H.E.S.S. data, showed a small excess of visible signal above 100 TeV that would be eventually visible in several years of operation of a future GNN infrastructure. Within the proposed hadronic scenario we linked the studied gamma-ray spectra with the luminosity of accelerating protons in the jet and in the lobes of M87. Considering as upper limit what has been observed up to now by TA experiment we were able to put some constraints on the density of M87 lobes for different sizes. In particular we found that the density ranges from 10^{-8} cm^{-3} to 10^{-3} cm^{-3} for a lobe size in the range $1 \text{ kpc} < R < 100 \text{ kpc}$.

ACKNOWLEDGEMENTS

We would like to thank Michelle Hui, Matthias Beilicke, Alba Fernandez, Fabrizio Tavecchio and Karsten Berger for sharing with us the data samples used in their publications about the M87 TeV emission. Also we thank Francis Halzen, William Lee, Antonio Stamerra and Steven Neil Shore for useful discussions and the TOPCAT team for the useful sky-map tools. This work was supported by Luc Binette scholarship and the projects IG100414, Conacyt 101958 and PAPIIT IN-108713.

REFERENCES

- Abdo, A. A. e. a. 2009, *ApJ*, 707, 55
Abramowski, A., Acero, F., Aharonian, F., et al. 2012, *ApJ*, 746, 151
Abu-Zayyad, T., & et al. 2012, *Nuclear Instruments and Methods in Physics Research A*, 689, 87
Acciari, V. A. e. a. 2010, *ApJ*, 716, 819
Aharonian, F. A. 2002, *MNRAS*, 332, 215
Aharonian, F. e. a. 2006, *Science*, 314, 1424
Aleksić, J., & et al. 2012, *A&A*, 544, A96
Atoyan, A. M., & Dermer, C. D. 2003, *ApJ*, 586, 79
Bahcall, J., & Waxman, E. 2001, *Phys. Rev. D*, 64, 023002
Barr, G. D., Gaisser, T. K., Lipari, P., Robbins, S., & Stanev, T. 2004, *Phys. Rev. D*, 70, 023006
Barr, G. D., Robbins, S., Gaisser, T. K., & Stanev, T. 2006, *Phys. Rev. D*, 74, 094009
Becker, J. K. 2008, *Phys. Rep.*, 458, 173
Beilicke, M., Aharonian, F., Benbow, W., & et al. 2008, *International Cosmic Ray Conference*, 3, 937
Biretta, J. A., Stern, C. P., & Harris, D. E. 1991, *AJ*, 101, 1632
de Gasperin, F., Orrù, E., Murgia, M., et al. 2012, *A&A*, 547, A56
Dermer, C. D., & Menon, G. 2009, *High Energy Radiation from Black Holes: Gamma Rays, Cosmic Rays, and Neutrinos*
Despringre, V., Fraix-Burnet, D., & Davoust, E. 1996, *A&A*, 309, 375
Fraija, N. 2014a, *ApJ*, 783, 44
—. 2014b, *MNRAS*, 441, 1209
Fraija, N., González, M. M., & Pérez, M. 2012a, in *-Ray Bursts 2012 Conference (GRB 2012)*
Fraija, N., González, M. M., Perez, M., & Marinelli, A. 2012b, *ApJ*, 753, 40
Halzen, F. 2007, *Ap&SS*, 309, 407
Hardcastle, M. J., Cheung, C. C., Feain, I. J., & Stawarz, Ł. 2009, *MNRAS*, 393, 1041
Hillas, A. M. 1984, *ARA&A*, 22, 425
Mei, S., Blakeslee, J. P., Côté, P., et al. 2007, *ApJ*, 655, 144
Moharana, R., & Gupta, N. 2009, *J. Cosmology Astropart. Phys.*, 8, 5
Raue, M., & Mazin, D. 2008, *International Journal of Modern Physics D*, 17, 1515
Rieger, F. M., Bosch-Ramon, V., & Duffy, P. 2007, *Ap&SS*, 309, 119
Ryu, D., Das, S., & Kang, H. 2010, *ApJ*, 710, 1422
Sommers, P. 2001, *Astroparticle Physics*, 14, 271
Sparks, W. B., Biretta, J. A., & Macchetto, F. 1996, *ApJ*, 473, 254
Stanev, T. 1997, *ApJ*, 479, 290
Swank, J. H. 2006, *Advances in Space Research*, 38, 2959
Tan, J. C., Beuther, H., Walter, F., & Blackman, E. G. 2008, *ApJ*, 689, 775
Waxman, E. 1998, in *19th Texas Symposium on Relativistic Astrophysics and Cosmology*, ed. J. Paul, T. Montmerle, & E. Aubourg
Waxman, E., & Bahcall, J. 1997, *Phys. Rev. Lett.*, 78, 2292
Waxman, E., & Bahcall, J. 1999, *Phys. Rev. D*, 59, 023002
Young, A. J., Wilson, A. S., & Mundell, C. G. 2002, *ApJ*, 579, 560

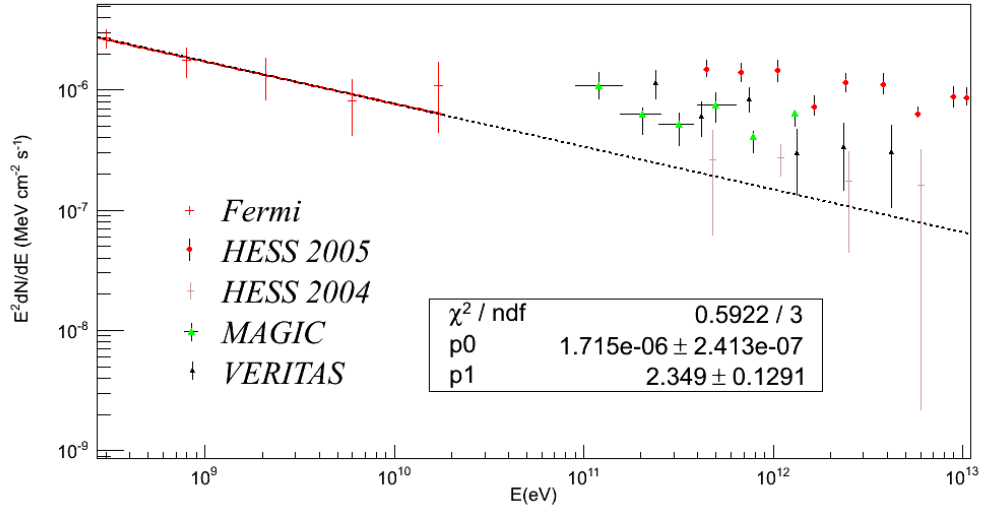


FIG. 1.— SED of M87 from 300 MeV up to more than 10 TeV. The parameters of the fit of Fermi data are reported as a p_0 (proportionality constant) and p_1 (spectral index). It is evident from this plot that only the one-zone SSC model used by the Fermi collaboration cannot be used to fit at the same time Fermi data and the reported TeV campaigns of MAGIC, VERITAS and H.E.S.S.

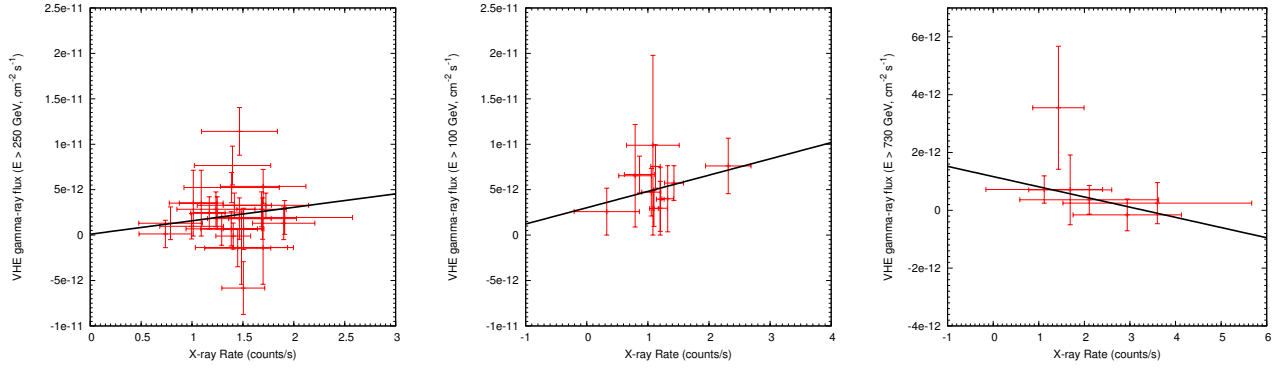


FIG. 2.— X-ray/VHE γ -ray correlation, obtained with X-ray data from RXTE/ASM and γ -ray data from VERITAS (left panel), MAGIC (central panel) and H.E.S.S. (right panel)

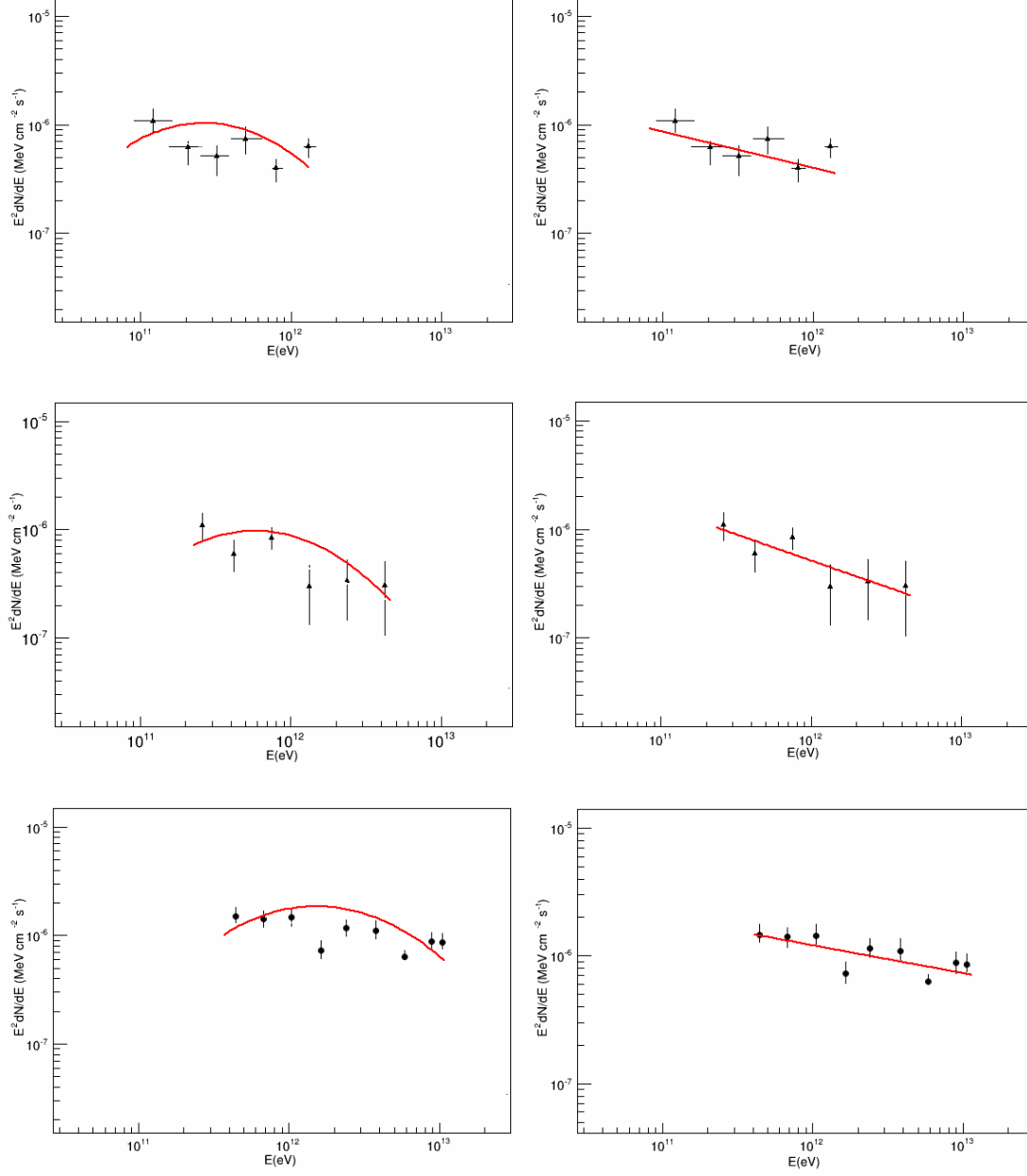


FIG. 3.— Best fit of the SED data reported by MAGIC, VERITAS and H.E.S.S. from top to bottom. The left column represents the proton-photon interaction model with the parameters reported in table A1 while the right column represents the proton-proton interaction model with the parameters reported in table A2.

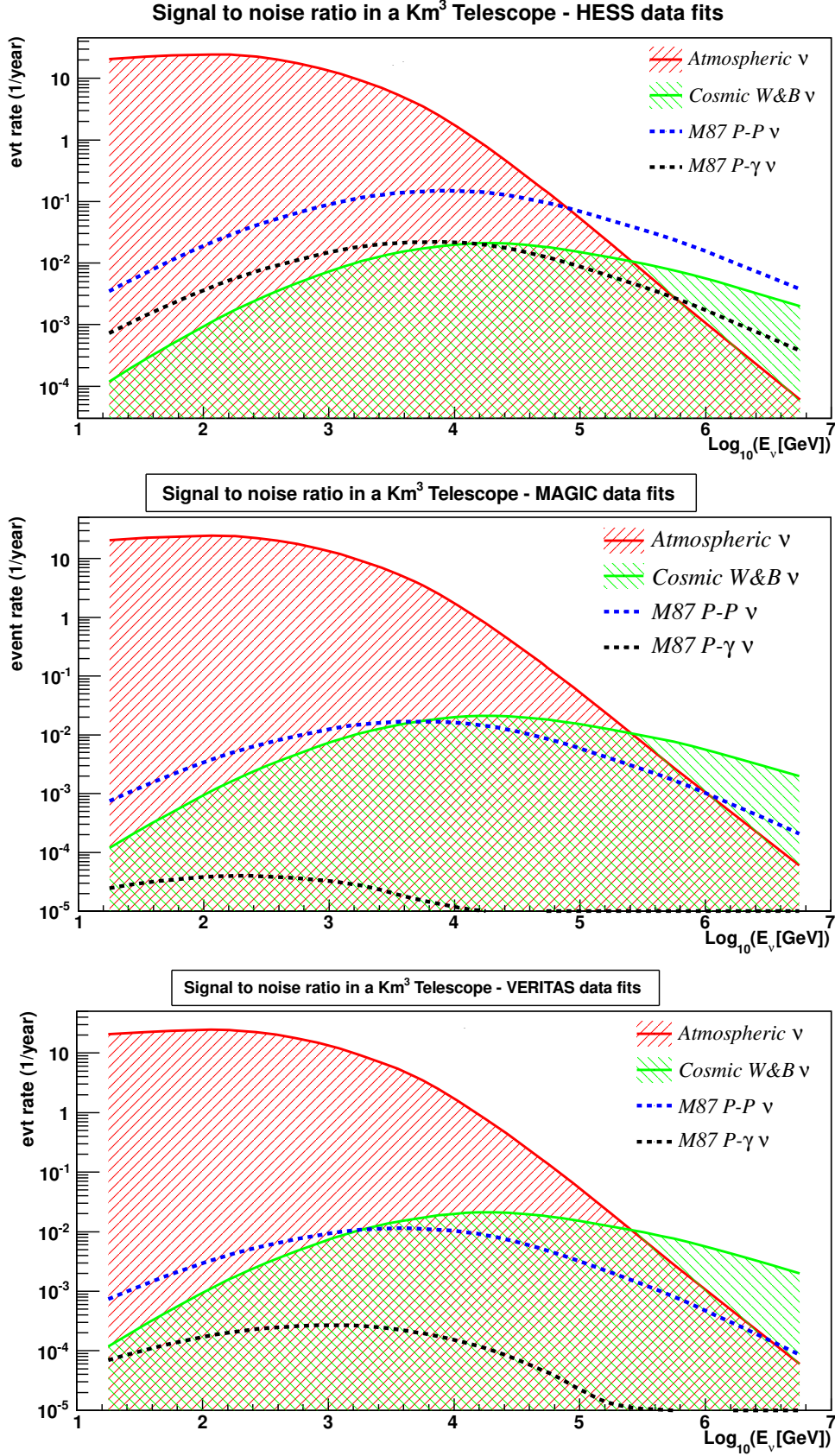


FIG. 4.— Neutrino signal to noise ratio for a Km³ northern neutrino telescope considering the M87 SEDs reported by H.E.S.S., MAGIC and VERITAS from top to bottom. The red and the green areas represent the atmospheric and diffuse neutrino “background” considered in this work in the region of 1° around M87 position; while blue and black dotted lines represent the neutrino signal produced by pp and p γ interactions respectively.

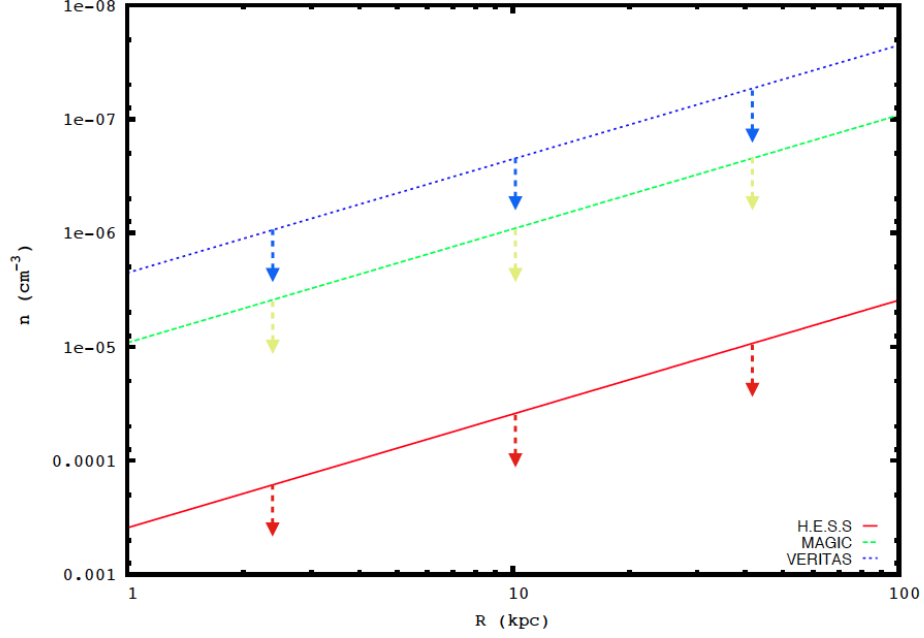


FIG. 5.— Lower limit of thermal particle density as a function of Lobes distance considering the pp model and the observations made by TA experiment in 5 years of observation. Less than one UHECR event possibly related with M87 position has been considered for this calculation.

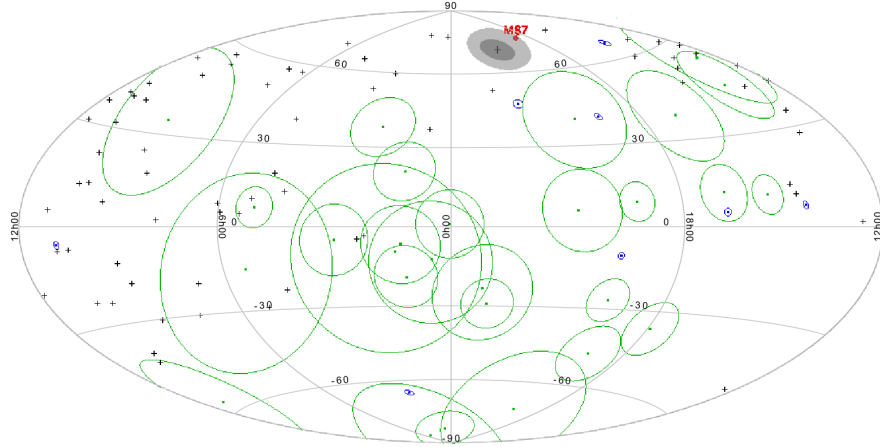


FIG. 6.— Sky map in galactic coordinates: with blue points are reported the neutrino track events reported by IceCube experiment and the respective errors (blue circles), with green points and green circles the neutrino shower events with the respectively directional errors represented by the green circles. With the black crosses are reported the cosmic ray events reconstructed by TA experiment above 57 EeV in 5 years. For the closest UHECR event to the M87 position we reported two grey contour region related to the possible deviation from the original direction due to the galactic and extragalactic magnetic fields, the inner one represent a deviation from the original direction of 5° while the surrounding one represent a deviation of 10° .